An Asymptotic Framework for the Analysis of Hydraulic Fractures: The Impermeable Case

S. L. Mitchell[1]
e-mail: sarah@iam.ubc.ca

R. Kuske

A. P. Peirce

Department of Mathematics,
University of British Columbia,
Vancouver, BC, V6T 1Z2,
Canada

This paper presents a novel asymptotic framework to obtain detailed solutions describing the propagation of hydraulic fractures in an elastic material. The problem consists of a system of nonlinear integro-differential equations and a free boundary problem. This combination of local and nonlocal effects leads to transitions on a small scale near the crack tip, which control the behavior across the whole fracture profile. These transitions depend upon the dominant physical process(es) and are identified by simultaneously scaling the associated parameters with the distance from the tip. A smooth analytic solution incorporating several physical processes in the crucial tip region can be constructed using this new framework. In order to clarify the exposition of the new methodology, this paper is confined to considering the impermeable case in which only the two physical processes of viscous dissipation and structure energy release compete.
[DOI: 10.1115/1.2200653]

1 Introduction

Hydraulic fracturing involves the propagation of a fracture in a brittle material, such as rock, due to the pressure exerted on the fracture surfaces by a viscous fluid that is pumped into the fracture. Hydraulic fractures occur naturally as a result of magma driven flows [1–3] as well as in several industrial and environmental applications such as the deliberate propagation of fractures in oil and gas reservoirs to enhance oil recovery; the generation of free-surface parallel hydraulic fractures in block caving mining operations as an alternative to explosive blasting [4]; and the generation of hydraulic fractures that are subsequently filled with impermeable material to isolate toxic waste or environmentally sensitive regions.

In many of these applications it is important to determine the progress of the fracture surface over time, which cannot be obtained from the few quantities that can easily be monitored, such as the fluid volume and pressure. It is, therefore, desirable to develop mathematical models that will predict the evolution of hydraulic fractures under given pumping conditions and geological situations [3,5–14]. The objective of these models is to calculate the fluid pressure, fracture width, and footprint given the properties of the rock, the injection rate, and the fluid characteristics. These models typically assume that: (i) the intact rock is linear elastic having a Young's modulus E and a Poisson's ratio ν; (ii) the fluid has viscosity μ; (iii) the progress of the fracture is controlled by rock toughness K_{Ic}; (iv) the loss of fluid to the reservoir (not considered in this paper) is determined by the leak-off coefficient C_l.

While the most general hydraulic fracture situations require numerical solution of these models, analytic and asymptotic methods also provide solutions for simple geometries. The highly nonlinear terms in the fluid flow equations, the nonlocal elastic response of the fracture, and the history-dependence of a sink term governing the fluid-loss present considerable challenges to mathematical

analysis. The analytic solutions are important as they provide: benchmarks against which to test numerical algorithms; detailed information about the singular near-tip behavior of the solution in order to design suitable basis functions for numerical models; and the parameter values and length scales that characterize the transitions between distinct combinations of physical processes.

The purpose of this paper is to present a novel asymptotic framework that enables us to determine the different propagation regimes as well as an asymptotic solution. The ultimate strength of the new methodology is its capacity for developing asymptotic solutions when more than two physical processes compete or, for situations in which the solution is not self-similar, for example, when a fracture passes through a bi-material interface. For clarity of exposition of the new methodology we concentrate here on self-similar solutions as in [15], in which only two physical processes (viscosity and toughness) compete.

The fracture geometry considered here, known as the KGD (plane strain) model, was developed independently by Geertsma and de Klerk [8] and Khristianovic and Zheltov [12]. It assumes the fracture is an infinite vertical strip so that horizontal cross-sections are in a state of plane strain, see Fig. 1. This model is applicable to large aspect ratio rectangular planar fractures and was extended in [16] to toughness. A major contribution to this mathematical modeling was by Spence and Sharp [16] who initiated the work on self-similar solutions and scaling for a KGD crack propagating in an elastic, impermeable medium with finite toughness. Their approach has been continued through asymptotic analyses of near-tip processes, yielding results for zero-toughness in an impermeable rock [17]; and for zero-toughness when leak-off is dominant [18]. Several papers [19–21] have extended this analysis to include toughness and fluid lag, where regions devoid of fluid develop close to the crack tip, along with transitional regions. This paper assumes that fluid lag is negligible and so these effects can be ignored.

Certain phases of hydraulic fracture propagation are characterized within a dimensionless parametric space [15,22], with boundaries controlled by the dominant processes, namely viscosity, energy release/toughness, or leak-off. This framework has been the basis for semi-analytical solutions for simple geometries (KGD and penny-shaped) which have provided benchmarks for numerical simulators. These include the following asymptotic regimes: impermeable with zero toughness [23–25], small toughness [26], finite toughness [16,27], and large toughness [25,28]; and permeable with zero toughness [29].
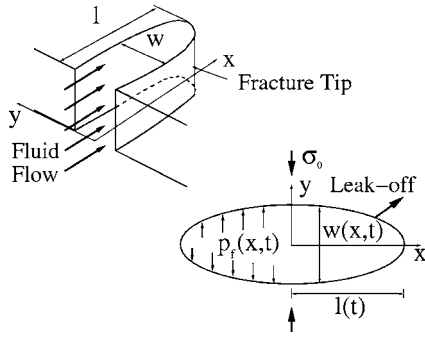

Fig. 1   The KGD profile and its cross-section

The analysis in this paper is closely related and complementary to these most recent studies; thus we describe here how our framework is different and more far-reaching. Previous analyses [21,23,24,26,28,30] have been limited to parameter regimes in which one or two physical processes dominate the dynamics, with the remainder of the related nondimensional quantities set to zero. A different set of scaling parameters is defined depending on which process is dominant, corresponding to the edges and corners of the parameter space [22,31]. We develop an asymptotic method which handles different scaling limits within a single framework, and so it is not necessary to redefine scaling parameters to consider the effect of different dominant processes. Although this study also only considers two physical processes, our analysis can be directly applied in situations where several processes are in balance, for example, including leak-off [32]. It can also be extended to other geometries, such as the PKN model [33], which assumes an elliptical vertical cross-section in contrast to the KGD model.

We avoid the semi-infinite approximations used in previous studies and consider parameter regimes which allow an asymptotic expansion with self-similar solutions. The method involves the simultaneous scaling of the physical processes relative to a parameter denoting the distance from the tip. A uniform asymptotic solution is then constructed in the tip region by rescaling the governing equations in terms of this small parameter. We determine the regions where the different processes are dominant, and relate them back to physical space. The process also identifies an important parameter combination quantifying these spatial transitions, which is used to match the local expansions analytically. This is in contrast to [26], where matching is done numerically. We find that the flexibility of the method is valuable for understanding the nonlocal and local effects in the model.

1.1   Governing Equations. We describe the governing equations for the propagation of an impermeable, KGD fracture driven by a viscous fluid in a uniform elastic medium under conditions of plane strain, as shown in Fig. 1. The solution is constructed to determine the fracture opening $w(x,t)$, net pressure $p(x,t)$ (the difference between the fluid pressure p_f and the far-field stress σ_0), and the fracture half-length, $l(t)$. We define three combined parameters E', μ', and K', in terms of the material parameters E, ν, μ, and K_{Ic}, as

$$E' = \frac{E}{1-\nu^2}, \quad \mu' = 12\mu, \quad K' = 4\left(\frac{2}{\pi}\right)^{1/2} K_{Ic} \qquad (1)$$

Along with the volumetric fluid injection rate Q_0, these parameters govern the fracture propagation. Consistent with linear elastic fracture mechanics, we assume that the rock toughness K_{Ic} equals the stress intensity factor K_I, which, for a symmetric crack in a state of plane strain subjected to a pressure p, is given by

$$K_{Ic} = K_I := 2\sqrt{\frac{l}{\pi}} \int_0^l \frac{p}{\sqrt{l^2 - x^2}} dx \qquad (2)$$

The governing equations are given as follows: The conservation of the fluid mass for an incompressible fluid with zero leak-off is described by the *lubrication equation*

$$\frac{\partial w}{\partial t} = \frac{1}{\mu'} \frac{\partial}{\partial x}\left[w^3 \frac{\partial p}{\partial x} \right] + Q_0 \delta(x) \qquad (3)$$

For a state of plane strain, the *elasticity equation*

$$p(x,t) = -\frac{E'}{4\pi} \int_{-l}^{l} \frac{\partial w}{\partial s} \frac{\mathrm{d}s}{s-x} \qquad (4)$$

expresses the force balance through a nonlocal relationship between the fracture opening and the net pressure. Equations (2) and (4) imply the local *propagation condition*

$$w = (K'/E')\sqrt{l-x} + O[(l-x)^{3/2}], \quad x \to \pm l \qquad (5)$$

which determines the asymptotic behavior of the fracture opening close to the tip. Finally, we have *boundary conditions*, which ensure zero width and zero fluid loss at the tip

$$w = 0, \quad w^3 \frac{\partial p}{\partial x} = 0, \quad \text{at } x = \pm l \qquad (6)$$

The *global volume balance condition*

$$Q_0 t = \int_{-l}^{l} w(s,t)\mathrm{d}s \qquad (7)$$

results from integrating (3) and using (6). The solution is constructed asymptotically by alternatively solving the lubrication equation (3) and the elasticity equation (4). In the near-tip region the dominant physical process is the energy release which is captured by the propagation condition (5). The remaining unknown constants are then found by applying the global volume balance condition (7); this also confirms the balance of dominant physical processes that arise.

1.2   Scaling and Dimensionless Equations. We seek a self-similar solution in the form $w(x,t) \propto l(t)\Omega(x/l,t)$ and, therefore, write the governing Eqs. (3)–(7) with nondimensionalized width, pressure and length scales

$$\xi = x/l, \quad l = L\gamma, \quad w = \epsilon L\Omega, \quad p = \epsilon E'\Pi \qquad (8)$$

as used in [31,28,26]. The nondimensional quantities Ω (the opening), Π (the net pressure), and γ (a fracture length) are all $O(1)$. The parameter ϵ is introduced here for comparison with [26,28,31], where it is used to relate w/l to p/E'. However, it could be set to unity in our analysis. The parameter L denotes a length scale and is of the same order as l. We assume that γ =constant in our analysis below and show that this assumption is valid in Sec. 2.5, for the impermeable case of zero leak-off.

The three nondimensional quantities, which play important roles in our analysis, are

$$\mathcal{G}_k = \frac{K'}{\epsilon E' L^{1/2}}, \quad \mathcal{G}_m = \frac{\mu'}{\epsilon^3 E' t}, \quad \mathcal{G}_v = \frac{Q_0 t}{\epsilon L^2} \qquad (9)$$

representing toughness/energy release, viscosity, and injected fluid volume, respectively. We simultaneously balance these parameters with the distance from the tip which allows us to consider regimes where both toughness and viscosity compete. The method can also be extended to consider multiple competing physical processes in balance, as in [32] where leak-off is included. Note that we have not introduced a nondimensionalized time scaling since it does not affect this balance approach. Here we examine the case where $\mathcal{G}_k \neq 0$ and $\mathcal{G}_m \neq 0$; the analysis for $\mathcal{G}_m = 0$ is the so called Griffiths crack solution [34], and $\mathcal{G}_k = 0$ is the viscosity solution [17,26].

The governing Eqs. (3)–(7) can, therefore, be written as

$$\frac{t(\epsilon L)_t}{\epsilon L}\Omega + t\frac{\partial\Omega}{\partial t} - \xi\frac{t(L\gamma)_t}{L\gamma}\frac{\partial\Omega}{\partial\xi} = \frac{1}{\mathcal{G}_m}\frac{1}{\gamma^2}\frac{\partial}{\partial\xi}\left[\Omega^3\frac{\partial\Pi}{\partial\xi}\right] \qquad (10)$$

$$\Pi = -\frac{1}{4\pi\gamma}\int_{-1}^{1}\frac{\partial\Omega}{\partial\chi}\frac{d\chi}{\chi-\xi} \qquad (11)$$

$$\Omega = \mathcal{G}_k\gamma^{1/2}(1\mp\xi)^{1/2}, \quad \xi\to\pm1 \qquad (12)$$

$$\mathcal{G}_v = \gamma\int_{-1}^{1}\Omega d\chi \qquad (13)$$

$$\Omega = 0, \quad \text{at } \xi = 1^{\pm} \qquad (14)$$

We determine different local expansions depending on which physical process is dominant, and then construct a uniform near-tip solution analytically. The regions where these expansions are valid depend on a critical parameter which is a combination of the dimensionless $\mathcal{G}_{()}$ quantities (9), and the transition in behavior can be related to the dominant physical processes. We determine this parameter as part of the process by scaling Eqs. (10)–(14) with a parameter controlling the distance from the tip $\xi=1$. Our method relies on analyzing the governing equations in this nondimensional form but we also quote the results in the original dimensional variables at the end of Sec. 2 to more easily give a physical interpretation.

Some of the expansions in this paper have been found previously, see [16,17,26,28,31] for example. We obtain the well-known results that the fracture width has $(1-x/l)^{1/2}$ and $(1-x/l)^{2/3}$ asymptotic behavior for the toughness and viscosity dominated regions, respectively. We also show that the fracture grows as $t^{2/3}$ and the fracture width is proportional to $t^{1/3}$. Although we confirm previous work, our new approach gives the construction in a transition region, where the solution consists of several terms in the expansion and thus is not purely a power law. It is also has the flexibility to handle behavior dominated by different physical processes simultaneously. When considering two or more physical processes, we do not rely on a scaling in which any one process is dominant: This is in contrast to other studies, [26,28,31] amongst others, where the nondimensional quantities $\mathcal{G}_{()}$ corresponding to the controlling processes are set to unity. In our method the critical parameters are determined as part of the expansion. In Sec. 2 we describe the approach of the method in detail and in Sec. 3 we briefly describe how the methodology can be extended to include leak-off and in [33] it is applied to the PKN model.

2 Analytical Solution Method

We now describe the new approach, which provides a unified framework to balance viscosity and toughness simultaneously.

2.1 Re-scaled Equations and Balancing Approach. First we scale the key dimensionless quantities in (9) with a parameter $\delta \ll 1$ related to the distance from the tip $\xi=1$. Then we define an asymptotic expansion for both Ω and Π in terms of this parameter, and balance δ with the nondimensionless quantities $\mathcal{G}_{()}$ (9). Through this procedure we can locate changes in the behavior of the solution and the spatial regions characterized by the different dominant physical processes. Thus we define

$$1 - \delta z = \xi \qquad (15)$$

$$\mathcal{G}_k = \delta^{\beta_k}\hat{\mathcal{G}}_k, \quad \mathcal{G}_m = \delta^{\beta_m}\hat{\mathcal{G}}_m, \quad \mathcal{G}_v = \delta^{\beta_v}\hat{\mathcal{G}}_v \qquad (16)$$

where the $\hat{\mathcal{G}}_{()}$ quantities are all $O(1)$. The construction of the asymptotic expansion determines inequalities between the values of the exponents $\beta_{()}$, which characterize the different regimes. The parameter $\delta \ll 1$ is essentially the distance from the tip, since

we assume that z is $O(1)$. Previous work, for example [26,28,31], assumes a semi-infinite approximation; however, the parameter δ allows us to be more general in the analysis of the fracture tip behavior as we have not assigned the exact distance from the tip. The semi-infinite approximation does not allow extensions to include stress jumps, for example, whereas the methodology described in this paper can incorporate such modifications. Note that the parameter δ is used for bookkeeping to balance terms in the expansion, but does not appear in the final solution.

We assume that the solution is symmetric about $\xi=0$ (see Fig. 1) and so, without loss of generality, we consider the interval $0 < \xi < 1$. Then the integral in (11) is written as (and similarly for the integral in (13))

$$\Pi = -\frac{1}{4\pi\gamma}\int_{-1}^{1}\frac{d\Omega}{d\chi}\frac{d\chi}{\chi-\xi} = -\frac{1}{2\pi\gamma}\int_{0}^{1}\frac{d\Omega}{d\chi}\frac{\chi d\chi}{\chi^2-\xi^2} \qquad (17)$$

The governing Eqs. (10)–(14) are now written in terms of z by substitutions of (15) and (16)

$$\frac{t(\epsilon L)_t}{\epsilon L}\Omega + (1-\delta z)\frac{t(L\gamma)_t}{L\gamma}\delta^{-1}\frac{d\Omega}{dz} = \frac{\delta^{-\beta_m-2}}{\hat{\mathcal{G}}_m\gamma^2}\frac{d}{dz}\left[\Omega^3\frac{d\Pi}{dz}\right] \qquad (18)$$

$$\Pi = -\frac{1}{2\pi\gamma}\delta^{-1}\int_{0}^{1/\delta}\frac{d\Omega}{dr}\frac{(1-\delta r)}{r(2-\delta r)-z(2-\delta z)}dr \qquad (19)$$

$$\Omega = \hat{\mathcal{G}}_k\gamma^{1/2}\delta^{\beta_k+1/2}z^{1/2}, \quad z\to0 \qquad (20)$$

$$\delta^{\beta_v}\hat{\mathcal{G}}_v = 2\gamma\delta\int_{0}^{1/\delta}\Omega dr \qquad (21)$$

$$\Omega = 0, \quad \text{at } z = 0 \qquad (22)$$

As mentioned above, we expand Ω and Π in terms of δ. The terms in these expansions can then be combined with the powers of δ appearing explicitly in (18)–(22). Hence we set

$$\Omega = \delta^{\beta_k+1/2}(\Omega_0 + \delta^{\alpha_1}\Omega_1 + \cdots) \qquad (23)$$

$$\Pi = \delta^{\beta_k}\Pi_0 + \delta^{\sigma_1}\Pi_1 + \cdots \qquad (24)$$

The exponents α_i and σ_i are unknown at present and determined below in terms of the exponents $\beta_{()}$ in (16) as part of the asymptotic construction. The method involves substituting (23) and (24) into (18)–(22) and matching terms in powers of δ using the exponents $\beta_{()}$. This determines the exponents α_i and σ_i and shows how the relative magnitudes of the dimensionless parameters (9) compared with δ influences the solution.

The sign of α_1 determines the leading order behavior of the solution, and we see more clearly how this arises in the expansions (23) and (24) by considering the lubrication Eq. (18). The leading order terms in δ satisfy

$$\lambda\delta^{-1}\frac{d\Omega}{dz} = \frac{1}{\hat{\mathcal{G}}_m\gamma^2}\delta^{-\beta_m-2}\frac{d}{dz}\left[\Omega^3\frac{d\Pi}{dz}\right] \qquad (25)$$

where we have assumed that the length scale L satisfies $L=C_L t^{\lambda}$.

The two situations which arise are either (i) the right-hand side of (25) is dominant and thus set to zero, so that to leading order Π=constant, and Ω is determined using the propagation condition (20). This corresponds to $\alpha_1>0$ and so Ω_0 is dominant and obtained from the propagation condition (20) which gives the classical square root term associated with a dominant toughness [28,31]. This in turn also defines Π_0 via (19). Note that the prefactor δ^{β_k} incorporated explicitly in (23) and (24) comes from the dimensionless toughness $\mathcal{G}_k$. Also, we show below that the other solution in (25), namely $\Omega^3\Pi'$=constant, cannot arise. Or, (ii) the two terms in Eq. (25) balance. This corresponds to $\alpha_1<0$ where

viscosity dictates the leading order behavior of $z^{2/3}$, as in [17,26,31] and discussed here in Sec. 2.3. Then the leading order terms in (23) and (24) are Ω_1 and Π_1, and we find that $\Omega_0, \Pi_0 = 0$. Hence the square root behavior is not leading order, implying that toughness is not dominant. Our expansion ties this change in leading order behavior to physical space.

To give the details and higher order terms of expansions (23) and (24) we substitute these expressions into the lubrication equation (18) to give

$$\frac{t(\epsilon L)_t}{\epsilon L} \delta^{\beta_k + 1/2}(\Omega_0 + \delta^{\alpha_1}\Omega_1 + \cdots) + \lambda(1 - \delta z)\delta^{\beta_k - 1/2}$$

$$\times \left(\frac{d\Omega_0}{dz} + \delta^{\alpha_1}\frac{d\Omega_1}{dz} + \cdots \right)$$

$$= \frac{\delta^{-\beta_m - 1/2 + 3\beta_k}}{\hat{\mathcal{G}}_m \gamma^2} \cdot \frac{d}{dz}\left[(\Omega_0 + \delta^{\alpha_1}\Omega_1 + \cdots)^3 \right.$$

$$\left. \times \left(\delta^{\beta_k}\frac{d\Pi_0}{dz} + \delta^{\sigma_1}\frac{d\Pi_1}{dz} + \cdots \right) \right] \quad (26)$$

and into the elasticity equation (19)

$$\delta^{\beta_k}\Pi_0 + \delta^{\sigma_1}\Pi_1 + \cdots = -\frac{\delta^{\beta_k - 1/2}}{2\pi\gamma} \cdot \int_0^{1/\delta} \left(\frac{d\Omega_0}{dr} + \delta^{\alpha_1}\frac{d\Omega_1}{dr} \right.$$

$$\left. + \cdots \right) \frac{(1 - \delta r)}{r(2 - \delta r) - z(2 - \delta z)}dr \quad (27)$$

In Secs. 2.2 and 2.3 we use (26) and (27) to determine local expansions in the different asymptotic limits, $\alpha_1 > (<)0$, by balancing terms according to powers of δ, and in Sec. 2.4 we match to obtain a uniform near-tip expansion. Finally, in Sec. 2.5 we substitute Ω from (23) into the global volume balance equation (21) to determine remaining unknown coefficients.

2.2 The Near-Tip Behavior ($\alpha_1 > 0$). First we look for an expansion where $\alpha_1 > 0$, and determine the conditions under which this is valid. The leading order terms in (26) and (27) for $\delta \ll 1$ are

$$0 = \frac{\delta^{-\beta_m - 1/2 + 4\beta_k}}{\hat{\mathcal{G}}_m \gamma^2}\frac{d}{dz}\left[\Omega_0^3\frac{d\Pi_0}{dz} \right] \quad (28)$$

$$\delta^{\beta_k}\Pi_0 = -\frac{\delta^{\beta_k - 1/2}}{2\pi\gamma}\int_0^{1/\delta}\frac{d\Omega_0}{dr}\frac{(1 - \delta r)}{r(2 - \delta r) - z(2 - \delta z)}dr \quad (29)$$

and the solution is determined as

$$\Omega_0(z) = C_0\sqrt{z(2 - \delta z)}, \quad \Pi_0(z) = \frac{C_0}{4\gamma} \quad (30)$$

where Π_0 is found by integrating (28) (see [32].) The solution (30) is the eigenfunction of (29) which, with $\Pi_0 = \text{constant}$, is symmetric about $\xi = 0$. It satisfies the propagation condition (20) to yield $C_0 = \hat{\mathcal{G}}_k\sqrt{\gamma/2}$. Comparison of the two leading terms in (26), namely the $\delta^{\beta_k - 1/2}$ and $\delta^{-\beta_m - 1/2 + 4\beta_k}$ terms, shows that we are in the toughness regime. We assume $\delta^{\beta_k - 1/2} < \delta^{-\beta_m - 1/2 + 4\beta_k}$ and then use (16) to deduce that $\mathcal{G}_k^3$ is large compared with $\mathcal{G}_m$, since the $\hat{\mathcal{G}}_0$ are $O(1)$. From the constant C_0 observe that the leading order term in the expansion for Ω (for $\alpha_1 > 0$) involves the re-scaled toughness parameter $\mathcal{G}_k$; this, together with the square root behavior, also implies that the toughness is dominant in this region. Note that we disregard the solution $\Omega_0^3\Pi_0' = \text{constant}$ in (28). Using the propagation condition (20) for Ω_0 implies that Π_0 is $O(z^{-1/2})$ to leading order, but this contradicts $\Pi_0 = \text{constant}$, which arises from (29).

The next order terms in (26) and (27) for $\delta \ll 1$ are

$$\lambda\delta^{\beta_k - 1/2}\frac{d\Omega_0}{dz} = \frac{\delta^{-\beta_m + 3\beta_k - 1/2 + \sigma_1}}{\hat{\mathcal{G}}_m\gamma^2}\frac{d}{dz}\left[\Omega_0^3\frac{d\Pi_1}{dz} \right] \quad (31)$$

$$\delta^{\sigma_1}\Pi_1 = -\frac{\delta^{\beta_k - 1/2 + \alpha_1}}{2\pi\gamma}\int_0^{1/\delta}\frac{d\Omega_1}{dr}\frac{(1 - \delta r)}{r(2 - \delta r) - z(2 - \delta z)}dr \quad (32)$$

Equating exponents of δ in (31) and (32) defines α_1 and σ_1 explicitly

$$\alpha_1 = 1/2 + \beta_m - 3\beta_k, \quad \sigma_1 = \beta_m - 2\beta_k \quad (33)$$

The condition $\alpha_1 > 0$ can be written as $\mathcal{G}_k^3/\mathcal{G}_m > \delta^{1/2}$, using (16), and violation of this condition means we are no longer in the toughness dominated regime.

We can now obtain Ω_1 and Π_1: Solving (31) gives

$$\Pi_1 = -\frac{C_1}{4\pi\gamma}\ln\left(1 - \frac{1}{2 - \delta z} \right) - \frac{C_1}{4\pi\gamma}[\ln(1 - \delta z) - \ln(\delta z)] \quad (34)$$

for $z = O(1)$, and then $\Omega_1(z) = C_1 z$ follows from (32). Note that the integration constant in (31) must be zero, otherwise Π_1 has infinite energy, deduced from integrating (31), also discussed in [32]: a non-zero constant means that Π_1 includes a $z^{-1/2}$ term, but substitution into the integral (2) would then yield an infinite stress intensity factor K_I. We can then find C_1 by substituting (34) into (31), considering the leading order terms only.

Hence the first two terms in the expansion (23) for Ω are

$$\Omega = \delta^{\beta_k}\hat{\mathcal{G}}_k\left[\sqrt{\frac{\gamma}{2}}\sqrt{\delta z(2 - \delta z)} + 4\pi\gamma^2\lambda\frac{\hat{\mathcal{G}}_m}{\hat{\mathcal{G}}_k^3}\delta^{\beta_m - 3\beta_k}(\delta z) \right] \quad (35)$$

which is valid when $\alpha_1 > 0$ or $\mathcal{G}_k^3/\mathcal{G}_m > \delta^{1/2}$, i.e., close to the tip for ξ near 1. The square root term is dominant, but in the transition region both terms in (35) become the same order, which is when toughness and viscosity balance.

2.3 The Intermediate-Tip Behavior ($\alpha_1 < 0$). The leading order terms in (26) for $\delta \ll 1$ are now

$$\lambda\delta^{\beta_k - 1/2 + \alpha_1}\frac{d\Omega_1}{dz} = \frac{\delta^{-\beta_m + 3\beta_k - 1/2 + 3\alpha_1 + \sigma_1}}{\hat{\mathcal{G}}_m\gamma^2}\frac{d}{dz}\left[\Omega_1^3\frac{d\Pi_1}{dz} \right] \quad (36)$$

which is coupled with the expression for Π_1 in (32). Equating exponents of δ in (32) and (36) gives

$$\alpha_1 = 1/6 + \beta_m/3 - \beta_k, \quad \sigma_1 = -1/3 + \beta_m/3 \quad (37)$$

The condition $\alpha_1 < 0$ then becomes $\mathcal{G}_k^3/\mathcal{G}_m < \delta^{1/2}$, which holds in the viscosity dominated regime; combining this with the analysis in Sec. 2.2 shows that the transition region occurs when $\mathcal{G}_k^3/\mathcal{G}_m = O(\delta^{1/2})$, and will be discussed in the following section.

Again we look for Ω_1 as a power law in z, namely

$$\Omega_1 = \bar{C}_1 z^m + \Omega_2 \quad (38)$$

where Ω_2 is a small correction term found below. This is equivalent to a perturbation expansion for the solution of (36) for $\Omega_2 \ll 1$, which we confirm in the matching.

The elasticity equation (32) can then be used to obtain

$$\Pi_1 = \cot\pi m\frac{\bar{C}_1 m}{4\gamma}z^{m-1} + \frac{\bar{C}_1 m\delta^{1-m}(2 - \delta z)^{-1}}{4\pi\gamma} + O(\delta^{1-m}) + \Pi_2 \quad (39)$$

where the leading term is the standard result for the integral (32) of Ω_1 for $\delta \to 0$, as given in [35] and discussed in the Appendix, and Π_2 is the term corresponding to Ω_2. We integrate (36) and substitute Ω_1 and Π_1 from (38) and (39), respectively; then the leading order terms are

$$\lambda \bar{C}_1 z^m = \frac{\bar{C}_1^4 \mu_m}{4\hat{\mathcal{G}}_m \gamma^3} z^{4m-2} \qquad (40)$$

where, for convenience, we have defined $\mu_m := m(m-1)\cot \pi m$. Equating exponents of z yields $m=2/3$ and the remaining expression determines $\bar{C}_1$. The equation for Ω_2 is then

$$\frac{\lambda d\Omega_2}{dz} = \frac{1}{\hat{\mathcal{G}}_m \gamma^2} \frac{d}{dz}\left[\frac{3\bar{C}_1^3 \mu_{2/3}}{4\gamma}\Omega_2 + \bar{C}_1^3 z^2 \frac{d\Pi_2}{dz}\right] \qquad (41)$$

We look for solutions to (41) of the form $\Omega_2 = \hat{\mathcal{A}}_1 z^h + \hat{\mathcal{A}}_2 z^p$, with Π_2 following directly from (32). Substitution of Ω_2 and Π_2 into (41) leads to

$$\lambda \hat{\mathcal{A}}_1 z^{(h-1)} + \lambda p \hat{\mathcal{A}}_2 z^p = \frac{h\bar{C}_1^3 \hat{\mathcal{A}}_1}{4\hat{\mathcal{G}}_m \gamma^3}[h(h-1)\cot \pi h + 3\mu_{2/3}]z^{h-1}$$
$$+ \frac{p\bar{C}_1^3 \hat{\mathcal{A}}_2}{4\hat{\mathcal{G}}_m \gamma^3}[p(p-1)\cot \pi p + 3\mu_{2/3}]z^{p-1} \qquad (42)$$

The coefficients $\hat{\mathcal{A}}_1$ and $\hat{\mathcal{A}}_2$ are unknown as they correspond to coefficients of homogeneous solutions to the linear Eq. (41). These are found below, by matching with (35). Setting $p=0$ gives one independent solution $\Omega_2 = \hat{\mathcal{A}}_2$. The other independent solution is found by solving a transcendental equation from matching the coefficients of z^{h-1} in (42). This reduces to

$$h(h-1)\cot \pi h + 2\mu_{2/3} = 0 \qquad (43)$$

We find that $h \approx 0.138673$, which confirms the result in [26]. The solution does not satisfy the $z^{1/2}$ behavior described by the propagation condition (20) for $\hat{\mathcal{G}}_k > 0$ (since $m \neq 1/2$ and $h \neq 1/2$), and so toughness is not dominant in the region where this solution holds. The terms Ω_0 and Π_0 are, therefore, set to zero in (23) and (24).

Then the first term in the expansion (23) for Ω is

$$\Omega = \delta^{\beta_m/3}\hat{\mathcal{G}}_m^{1/3}\left[\left\{\frac{4\gamma^3 \lambda}{\mu_m}\right\}^{1/3}(\delta z)^{2/3} + \frac{\hat{\mathcal{A}}_1 \delta^{2/3-h}}{\hat{\mathcal{G}}_m^{1/3}}(\delta z)^h + \frac{\hat{\mathcal{A}}_2 \delta^{2/3}}{\hat{\mathcal{G}}_m^{1/3}}\right] \qquad (44)$$

for $\alpha_1 < 0$ or $\mathcal{G}_k^3/\mathcal{G}_m < \delta^{1/2}$. This expression is valid only away from $\xi=1$, since the propagation condition (20) is not satisfied.

It should be noted that the next term in the expansion for Ω in (23), for $\alpha_1 < 0$, is given by $\Omega_2 = z^{5/3}$. It can be shown to be higher order in the construction of the uniform near-tip expansion and so is not included in (44).

2.4 Transition Region and Matching. We now consider the local expansions (35) for $\alpha_1 > 0$ and (44) for $\alpha_1 < 0$, to determine the transitions in spatial behavior, find the unknown coefficients by matching, and construct the uniform near-tip asymptotic expansion. Motivated by the balance Eqs. (33) and (37), we define a combined parameter $\mathcal{P}_{km}$ involving $\mathcal{G}_k$ and $\mathcal{G}_m$, namely

$$\mathcal{P}_{km} := \mathcal{G}_k^3/\mathcal{G}_m \qquad (45)$$

which appears explicitly in both expansions. These expansions can be written in the ξ scaling, without δ, in terms of $\mathcal{P}_{km}$ as

$$\Omega \sim \mathcal{G}_k[C_0\sqrt{1-\xi^2} + C_1 \mathcal{P}_{km}^{-1}(1-\xi)] \qquad (46)$$

$$\Omega \sim \mathcal{G}_m^{1/3}[\bar{C}_1(1-\xi)^{2/3} + \mathcal{A}_1(\mathcal{P}_{km})(1-\xi)^h + \mathcal{A}_2(\mathcal{P}_{km})] \qquad (47)$$

for $\alpha_1 > (<)0$, respectively. The coefficients C_0, C_1, and $\bar{C}_1$ have been re-defined without the $\hat{\mathcal{G}}_{()}$ terms as these are combined with
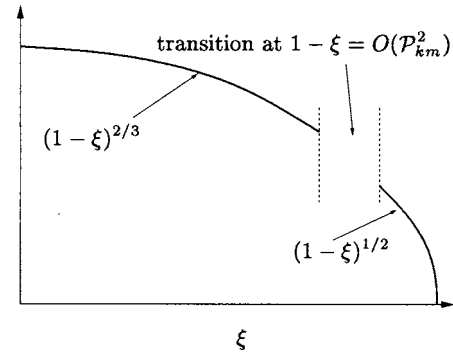

Fig. 2 Diagram of the solution Ω versus ξ near the fracture tip with transition region at $1-\xi=O(\mathcal{P}_{km}^2)$

$\delta^{\beta_{()}}$ to give the dimensionless $\mathcal{G}_{()}$. Also, the coefficients $\mathcal{A}_1(\mathcal{P}_{km})$ and $\mathcal{A}_2(\mathcal{P}_{km})$ are re-defined, observed by comparing (44) and (47). These depend on the parameter $\mathcal{P}_{km}$ since they are determined by matching (46) and (47) in a transition region which is related to $\mathcal{P}_{km}$, as discussed below. Some of the terms in (46) and (47) have also been found in previous work. The terms in (46) were given in [16,26,31], and also in [28] in the asymptotic limit of large toughness, with the second given for $x \to \pm l$, i.e., in limit close to the tip. The first term in (47) is found in [17], and the first two terms in (47) are used in local expansions in [26,31], in the asymptotic limit of small toughness as $x \to \pm l$. However, the constant term in (47) is not found in [26]. This new parameter is important in the matching, as shown below.

The definition of the parameter $\mathcal{P}_{km}$ follows naturally from the two different regimes where either toughness or viscosity dominates the behavior. These two regimes correspond to $\alpha_1 > (<)0$, as seen by re-examining (33) and (37). Recalling that $1-\xi=O(\delta)$, we can rewrite the condition on α_1 in terms of the physical parameters $\mathcal{G}_{()}$ and the distance from the tip. The solution for $\alpha_1 > 0$ is physically significant when toughness is dominant ($\mathcal{G}_k^3 \gg \mathcal{G}_m$), which in physical space is close to the tip and translates to $\mathcal{P}_{km} \gg (1-\xi)^{1/2}$. As $(1-\xi)^{1/2}$ approaches $\mathcal{P}_{km}$, the terms in (46) and (47) are the same order of magnitude; we observe a transition to an intermediate-tip region (see Fig. 2), which is found by considering $\alpha_1 < 0$ in (47). This is valid when the viscosity is dominant ($\mathcal{G}_k^3 \ll \mathcal{G}_m$), which in the physical space is away from the tip and translates to $\mathcal{P}_{km} \ll (1-\xi)^{1/2}$. Thus the expansion (46) holds for $1-\xi < \mathcal{P}_{km}^2$ and the expansion (47) for $1-\xi = O(\mathcal{P}_{km}^s)$, with $0 < s < 2$, and $\mathcal{P}_{km} \ll 1$.

The results confirm work carried out in [26] where the expansion is in terms of a parameter $\mathcal{K}^6 \ll 1$ with $\mathcal{G}_k = \mathcal{K}$ for $\mathcal{G}_v = \mathcal{G}_m = 1$; the relationship $\mathcal{P}_{km}^2 = O(1-\xi)$ can be shown to be equivalent to their scalings with $\mathcal{K}$. Also, our expansion for the toughness dominated solution (46) agrees with that found in [28] where a series expansion is obtained in terms of a parameter $\mathcal{M}$ with $\mathcal{G}_m = \mathcal{M}$ for $\mathcal{G}_v = \mathcal{G}_k = 1$. However, one difference between the two approaches is that in both [26,28] the matching is done by numerical calculation of a series expansion, while below we construct a uniform near-tip expansion analytically. The other main differences are that our framework can be extended to consider cases with more than two physical processes in balance, for example, including leak-off [32], and extended to cases in which the solution is not self-similar.

We construct a uniform near-tip asymptotic approximation by matching in the transition region where $\mathcal{G}_k^3/\mathcal{G}_m = O((1-\xi)^{1/2})$. In this region the leading order terms in the lubrication equation satisfy (25), coupled with the propagation condition (20). Note that both (46) and (47) are solutions of (25) in the two asymptotic limits. A closed form solution to (25) cannot be given in this
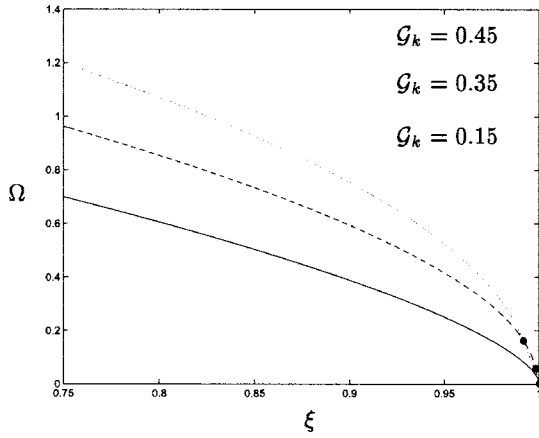
Fig. 3 Solution profiles of Ω versus ξ in the viscosity dominated regime with $\mathcal{G}_m = 1$ and $\mathcal{G}_k = 0.45, 0.35, 0.15$ (and so $\mathcal{P}_{km} = 0.091, 0.043, 0.003$)
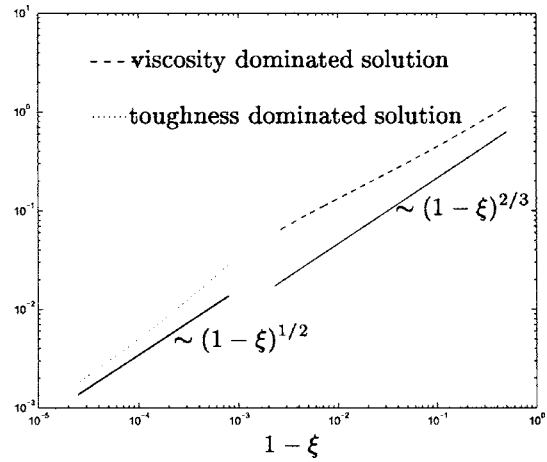

Fig. 4 Plot of $\log \Omega$ versus $\log(1-\xi)$ in the viscosity dominated regime with $\mathcal{G}_m = 1$, $\mathcal{G}_k = 0.35$ (and so $\mathcal{P}_{km} = 0.043$). The solid line denotes the leading order power law solutions, as indicated above.

region, but it can be constructed computationally where $1-\xi = O(\mathcal{P}_{km}^2)$ for $0 < \mathcal{P}_{km} \ll 1$, providing the basis for numerical matching in [26].

However, the identification of $\mathcal{P}_{km}$ and the correct form of Ω_2 allows us to determine the remaining unknown coefficients $\mathcal{A}_1(\mathcal{P}_{km})$ and $\mathcal{A}_2(\mathcal{P}_{km})$ to give an analytical expression for the matching. The critical scaling is $1-\xi = \mathcal{P}_{km}^2 \zeta$ for $\zeta = 0(1)$, and substitution into (46) and (47) yields, respectively

$$\Omega \sim \mathcal{G}_k [C_0 \mathcal{P}_{km} \zeta^{1/2} \sqrt{2 - \mathcal{P}_{km}^2 \zeta} + C_1 \mathcal{P}_{km} \zeta] \tag{48}$$

$$\Omega \sim \mathcal{G}_m^{1/3} [\bar{C}_1 \mathcal{P}_{km}^{4/3} \zeta^{2/3} + \mathcal{A}_1(\mathcal{P}_{km}) \mathcal{P}_{km}^{2h} \zeta^h + \mathcal{A}_2(\mathcal{P}_{km})] \tag{49}$$

Equating (48) and (49) and their first derivatives gives

$$\mathcal{A}_1(\mathcal{P}_{km}) = \frac{1}{h} \mathcal{P}_{km}^{-2h+4/3} \left[\frac{C_0}{\sqrt{2}} + C_1 - \frac{2\bar{C}_1}{3} \right] \tag{50}$$

$$\mathcal{A}_2(\mathcal{P}_{km}) = \mathcal{P}_{km}^{4/3} \left[\frac{(2h-1)\sqrt{2}C_0}{2h} + \frac{(h-1)C_1}{h} - \frac{(3h-2)\bar{C}_1}{3h} \right] \tag{51}$$

which is equivalent to writing a Taylor series for (46) and (47) about $1-\xi = O(\mathcal{P}_{km}^2)$ where Ω is regular, and matching the first two terms. The coefficient of the error is proportional to $\Omega''(\zeta)$ which is bounded for $\zeta = O(1)$ with respect to $\mathcal{P}_{km} \ll 1$, so that terms are matched up to $O(\mathcal{P}_{km}^{4/3})$. Figure 3 shows solution profiles of Ω against ξ for several values of $\mathcal{P}_{km}$. The location of the match point within the transition region is identified in the figure by asterisks enclosed in circles. The majority of the solution in these cases follows the 2/3 power law characteristic of the viscosity dominated propagation. To further emphasize this transition we provide a log-log plot of Ω in Fig. 4. The asymptotic 1/2 and 2/3 power law behaviors for the toughness and viscosity dominated regions can be clearly seen, while in the transition region the solution does not follow a simple power law.

The elasticity equation (19) determines Π, which is used above in the lubrication equation as part of the solution process. The corresponding expansions to (46) and (47) are

$$\Pi \sim \mathcal{G}_k \left[\Pi_0 - \mathcal{P}_{km}^{-1} \frac{C_1}{4\pi\gamma} \left\{ \ln \left| 1 - \frac{1}{1+\xi} \right| + \ln \left| \frac{1}{1-\xi} \right| + \ln \xi \right\} \right] \tag{52}$$

$$\Pi \sim \mathcal{G}_m^{1/3} \left[m \cot \pi m \frac{\bar{C}_1}{4\gamma} (1-\xi)^{m-1} + h \cot \pi h \frac{\mathcal{A}_1(\mathcal{P}_{km})}{4\gamma} (1-\xi)^{h-1} \right] \tag{53}$$

for $\mathcal{P}_{km} \gg (\ll)(1-\xi)^{1/2}$, respectively, and the calculations are outlined in the Appendix. In Fig. 5 we graph Π for different values of $\mathcal{P}_{km}$. Note that Π is a monotonically decreasing function of ξ in each case, which is consistent with gradient driven fluid flow and dynamic, viscosity driven, fracture propagation. However, as $\mathcal{G}_k$ is increased Π becomes close to a constant in spite of the fact that the propagation regime is considered viscous owing to the 2/3 power law behavior of Ω over the majority of the fracture. Indeed, this pressure profile is surprisingly close to that in the toughness dominated regime which is characterized by a zero pressure gradient to leading order owing to the quasi-static mode fracture propagation in a tough material. We also note the presence of the region close to the fracture tip where the pressure becomes negative. This "cavitation region" is an artifact of the model which deviates from the physical situation where the fluid front lags behind the fracture front. Such fluid lag regions, which can be significant in fractures propagating in low confinement environments, are beyond the scope of the model considered in this paper as the appropriate zero pressure boundary condition and unknown lag boundary would have to be included. The phenomenon of fluid
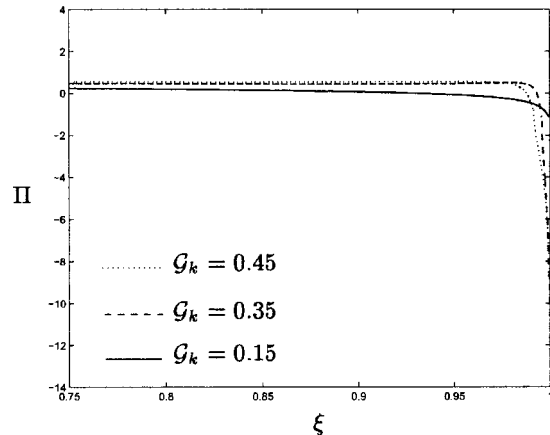

Fig. 5 Solution profiles of Π versus ξ corresponding to Ω in Fig. 3

lag has been studied analytically in [21,36] and numerically in [37], both for separate toughness and viscosity regimes, and analytically and numerically in [19] for the stationary problem with dominant toughness.

2.5 The Global Volume Balance Condition. We now use the global volume balance condition (13) to determine the dimensionless length parameter γ, defined in (8). The expression incorporates the dimensionless quantities $\mathcal{G}_{()}$ in (9) which involve powers of t. We can thus find the parameter λ, the power law exponent for $L=C_L t^\lambda$, with C_L constant, and justify the use of the self-similar solution. The condition also checks the ordering of the terms in the expansion. When $\mathcal{P}_{km}\gg1$, clearly $\mathcal{P}_{km}\gg(1-\xi)^{1/2}$ and the solution for Ω in (46) holds for all ξ. Then the global volume balance condition becomes

$$\mathcal{G}_v = \gamma\pi\mathcal{G}_k C_0/2 + \gamma\mathcal{G}_k C_1 \mathcal{P}_{km}^{-1} \tag{54}$$

In the limit $\mathcal{G}_m\rightarrow0$, the resulting value of γ in (54) agrees with the value obtained numerically in previous studies [31,28], which include computational results of Ω for $\xi\sim0$. We substitute $L=C_L t^\lambda$ into (54) using the definitions of $\mathcal{G}_v$ and $\mathcal{G}_k$ from (9), and the expression for C_1 from (35), to give

$$\frac{Q_0}{\epsilon C_L^2}t^{1-2\lambda} = \pi\left(\frac{\gamma}{2}\right)^{3/2}\frac{K'}{\epsilon E' C_L^{1/2}}t^{-\lambda/2} + 4\pi\gamma^3\frac{C_L^2\mu'E'}{\epsilon K'^2}t^{\lambda-1} \tag{55}$$

Then, in this toughness dominated regime, we find that $\lambda=2/3$.

Now we examine the situation $\mathcal{P}_{km}\ll1$, away from the toughness dominated regime, where the solution for Ω in (46) is valid for $1-\xi<\mathcal{P}_{km}^2$, and (47) is valid for $\mathcal{P}_{km}^s>1-\xi>\mathcal{P}_{km}^2$, for $0<s<2$. For the remainder of the integral (13), Ω must be computed numerically as in [23,26,31], yielding $\gamma\approx0.61524$, which is used in Figs. 4 and 5. Although a numerical approximation of the solution near $\xi=0$ is required to find γ, this computation is straightforward and the significance of our method is that we can obtain an analytical result for the solution near the tip, where numerical computation is more difficult.

For $\mathcal{P}_{km}\ll1$, the leading contribution to the integral in (13) is given by the part for ξ away from 1. For these values of ξ, the forms of the lubrication and elasticity equations indicate that Ω and Π must scale with $\mathcal{G}_m^{1/3}$, so that (13) reduces to $\mathcal{G}_v=\text{const}\cdot\mathcal{G}_m^{1/3}$. Substituting $L=C_L t^\lambda$ and the definitions of $\mathcal{G}_v$ and $\mathcal{G}_m$ from (9) then also yields $\lambda=2/3$. The time dependence of the leading order terms are all $t^{-1/3}$, confirming that the self-similar solution, with γ is constant, is appropriate to leading order. In practice if leak-off is included, this assumption could break down and some time dependence in γ may have to be considered, as discussed in [32].

We summarize the main results (46) and (47) in the original dimensional variables. For $\mathcal{P}_{km}:=(K'^3 t)/(\mu'E'^2 L^{3/2})\gg(\ll)(1-x/l)^{1/2}$, respectively

$$w \sim \frac{K'}{E'}l^{1/2}\left\{\left(1-\frac{x}{l}\right)^{1/2} + \frac{8\pi}{3}\gamma^{3/2}\mathcal{P}_{km}^{-1}\left(1-\frac{x}{l}\right)\right\} \tag{56}$$

$$w \sim \left(\frac{\mu'}{E'}\right)^{1/3}\frac{l}{t^{1/3}}\left\{2^{2/3}\sqrt{3}\left(1-\frac{x}{l}\right)^{2/3} + C_{11}\gamma^{-1}\mathcal{P}_{km}^{-2h+4/3}\left(1-\frac{x}{l}\right)^h\right.$$
$$\left. + C_{12}\gamma^{-1}\mathcal{P}_{km}^{4/3}\right\} \tag{57}$$

Observe that these expansions confirm the well-known results regarding the time dependence of the fracture, as discussed in [17,23]; the fracture half-length $l(t)$ is proportional to $t^{2/3}$ and, therefore, the dimensional fracture width w is proportional to $t^{1/3}$. Also, the spatial dependence in (56) and (57) agrees with previous work: the first two terms in both these expansions were obtained in [26]; the leading order terms in both and the second term in (57) (in the asymptotic limit $x\rightarrow\pm l$) were obtained in [31]; and

[28], which considers large toughness, obtained both terms in (56), again in the asymptotic limit $x\rightarrow\pm l$ for the latter. However, our analysis shows that the additional terms in (56) and (57) are needed to construct a uniform asymptotic near-tip solution between the two expansions.

3 Conclusions and Extensions

In this paper we have presented a new technique to analyze the system of integro-differential equations that arise when fluid-driven fractures are generated in an impermeable elastic solid. Our theoretical approach gives detailed solutions of the crack tip region and identifies the important processes controlling the fracture growth, namely viscosity and toughness. The combined parameter which quantifies these processes can be identified from critical scaling relationships between the nondimensional distance from the tip $1-\xi$ and the key nondimensional quantities $\mathcal{G}_k$, $\mathcal{G}_m$, and $\mathcal{G}_v$, representing toughness/energy release, viscosity, and injected fluid volume, respectively. This allows us to construct a uniform near-tip asymptotic expansion analytically instead of numerically as in [26]. From the expansion we can highlight the dominant physical processes through the parameter combination $\mathcal{P}_{km}=\mathcal{G}_k^3/\mathcal{G}_m$, relate these processes to the distance from the tip, and locate the transition region $\mathcal{P}_{km}=O((1-\xi)^{1/2})$.

It is straightforward to extend the method to the permeable case when leak-off is included. A similar analysis in [32] leads to expansions which we quote here in the original variables. For $\mathcal{P}_{ckm}:=(K'^4 t^{1/2})/(C'\mu'E'^3 L^{1/2})\gg(\ll)(1-x/l)^{1/2}$, respectively

$$w \sim \frac{K'}{E'}l^{1/2}\left\{\left(1-\frac{x}{l}\right)^{1/2} + \left[\frac{8\pi}{3}\gamma^{3/2}\mathcal{P}_{km}^{-1} + 4\sqrt{2}\pi\gamma\mathcal{P}_{ckm}^{-1}\right]\left(1-\frac{x}{l}\right)\right\} \tag{58}$$

$$w \sim \left(\frac{C'\mu'}{E'}\right)^{1/4}\frac{l^{3/4}}{t^{1/8}}\gamma^{-3/4}\left\{\tilde{C}_{01}\left(1-\frac{x}{l}\right)^{5/8} + \mathcal{B}_1\left(1-\frac{x}{l}\right)^{1/8}\right.$$
$$\left. + \mathcal{B}_2\left(\frac{\mu'\gamma^{-3}}{C'^3 E'}\right)^{1/4}\frac{l^{3/4}}{t^{5/8}}\left(1-\frac{x}{l}\right)^{3/4} + \mathcal{B}_3\left(1-\frac{x}{l}\right)^r\right\} \tag{59}$$

where C' is the leak-off parameter, and $\mathcal{P}_{ckm}$ is a combination of $\mathcal{G}_k$, $\mathcal{G}_m$, and the corresponding dimensionless leak-off parameter. Observe that the fracture width w is now proportional to $t^{1/4}$, as opposed to $t^{1/3}$ for zero leak-off, which is deduced using the result that the fracture grows as $t^{1/2}$ for the permeable case. The results in (58) and (59) are found from balancing these three parameters simultaneously with the distance from the tip. The coefficients $\mathcal{B}_1$ and $\mathcal{B}_3$, analogous to $\mathcal{A}_1$ and $\mathcal{A}_2$ in this study, are determined by matching in the transition region. The expansion (58) gives the toughness dominated limit, and is analogous to (47) with an extra leak-off term. The expansion in (59) gives the leak-off dominated limit, where the leading order 5/8 term was established by [18] for the stationary solution. The other terms in (59) are new and again necessary in order to match the expansions in the two limits analytically.

Our methodology has also been applied to fracture propagation with a finger-like geometry, known as the PKN fracture [13,14]. The results show a transition between $(1-\xi)^{1/3}$ and $(1-\xi)^{2/3}$ power laws which correspond to the leading terms in the far- and near-tip expansions for zero toughness [33].

Appendix: Calculation of Π

To calculate Π we substitute expansions (46) and (47) into the elasticity equation (17). A parameter ξ^* is introduced which is in the transition region $1 - \xi = O(P_{km}^2)$, for example $1 - \xi^* = P_{km}^2$. Then (17) becomes

$$\Pi = - \frac{\mathcal{G}_k}{4\pi\gamma} \int_{\xi^*}^1 \left\{ C_0[(1-\chi^2)^{1/2}]' + C_1 \mathcal{P}_{km}^{-1}[(1-\chi)]' \right\} \frac{2\chi \mathrm{d}\chi}{\chi^2 - \xi^2}$$
$$- \frac{\mathcal{G}_m^{1/3}}{4\pi\gamma} \int_0^{\xi^*} \left\{ \bar{C}_1[(1-\chi)^{2/3}]' + \mathcal{A}_1(\mathcal{P}_{km})[(1-\chi)^h]' \right\} \frac{2\chi \mathrm{d}\chi}{\chi^2 - \xi^2}$$
$$=: I_1 + I_2 \tag{A1}$$

Different asymptotic expansions for I_1 and I_2 are found depending on the position of ξ relative to the interval of integration. In the near-tip region $\xi > \xi^*$, the integral I_2 gives $O(1)$ terms and the leading order contribution comes from the singularity in I_1. Hence the near-tip expansion for Π is

$$\Pi \sim \mathcal{G}_k \left[\frac{C_0}{4\gamma} - \frac{C_1 \mathcal{P}_{km}^{-1}}{4\pi\gamma} \left\{ \ln \left| \frac{\xi^2 - \xi^{*2}}{1 - \xi^2} \right| \right\} \right]$$

for $\mathcal{P}_{km} \gg 1$, which to leading order corresponds to (52) with $\xi^* = 0$ in the correction.

For intermediate values $\xi < \xi^*$, the leading order expansion for Π comes from I_2 in (A1). Consider the general integral

$$J = \int_0^{\xi^*} \frac{(1-\chi)^{a-1}}{\chi - \xi} \mathrm{d}\chi - \int_{-\xi^*}^0 \frac{(1+\chi')^{a-1}}{\chi' - \xi} \mathrm{d}\chi' =: J^A + J^B$$

where $0 < a < 1$. Then the result for I_2 follows by setting $a = 2/3$ and $a = h$ in the integral J, since these exponents correspond to Π_1 and Π_2 from Sec. 2.3. Introducing variables $\delta Z = 1 - \xi$ and $\delta R = 1 - \chi$ means J^A can be written as

$$J^A = - \delta^{a-1} \left(\int_0^\infty - \int_{1/\delta}^\infty - \int_0^{(1-\xi^*)/\delta} \right) \frac{R^{a-1}}{R - Z} \mathrm{d}R \tag{A2}$$

Then the leading order contribution to Π in the intermediate-tip region $\xi < \xi^*$ is determined by the first integral in (A2) for $\delta = \mathcal{P}_{km}^2 \ll 1$, see [35]. Hence $J^A = (\delta Z)^{a-1} \pi \cot \pi a + O(1)$ and a similar calculation gives J^B. Thus

$$\Pi \sim \frac{\mathcal{G}_m^{1/3}}{4\gamma} \left\{ \frac{m \cot \pi m \bar{C}_1}{4\gamma}(1-\xi)^{m-1} + \frac{h \cot \pi h \mathcal{A}_1(\mathcal{P}_{km})}{4\gamma}(1-\xi)^{h-1} \right\}$$

for $\mathcal{P}_{km} \ll 1$, where $m = 2/3$ and $h \approx 0.138673$, and corresponds to leading order to (39).

References

[1] Lister, J. R., 1990, "Buoyancy-Driven Fluid Fracture: Similarity Solutions for the Horizontal and Vertical Propagation of Fluid-Filled Cracks," J. Fluid Mech., **217**, pp. 213–239.
[2] Lister, J. R., 1990, "Buoyancy-Driven Fluid Fracture: The Effects of Material Toughness and of Low-Viscosity Precursors," J. Fluid Mech., **210**, pp. 263–280.
[3] Spence, D. A., and Turcotte, D. L., 1985, "Magma-Driven Propagation of Cracks," J. Geophys. Res., **90**, pp. 575–580.
[4] Van As, A., and Jeffrey, R. G., 2000, "Caving induced by Hydraulic Fracturing at Northparkes Mines," in *Proc. 4th North American Rock Mechanics Symp.*, J. E. A. Girard, ed., pp. 353–360.
[5] Abé, H., Mura, T., and Keer, L. M., 1976, "Growth Rate of a Penny-Shaped Crack in Hydraulic Fracturing of Rocks," J. Geophys. Res., **81**, pp. 5335–5340.
[6] Barenblatt, G., 1962, "The Mathematical Theory of Equilibrium Cracks in Brittle Fracture," Adv. Appl. Mech., **7**, pp. 55–129.
[7] Crittendon, B. C., 1959, "The Mechanics of Design and Interpretation of Hydraulic Fracture Treatments," J. Pet. Technol., **11**(10), pp. 21–29.
[8] Geertsma, J., and de Klerk, F., 1969, "A Rapid Method of Predicting Width and Extent of Hydraulically Induced Fractures," J. Pet. Technol., **246**, pp. 1571–1581.
[9] Harrison, E., Kieschnick, W. F., and McGuire, W. J., 1954, "The Mechanics of Fracture Induction and Extension," Trans. Am. Inst. Min., Metall. Pet. Eng., **201**, pp. 252–263.
[10] Howard, G. C., and Fast, C. R., 1957, "Optimum Fluid Characteristics for Fracture Extension," Drill. & Prod. Prac., **24**, pp. 261–270.
[11] Hubbert, M. K., and Willis, D. G., 1957, "Mechanics of Hydraulic Fracturing," Trans. Am. Inst. Min., Metall. Pet. Eng., **210**, pp. 153–166.
[12] Khristianovic, S., and Zheltov, Y., 1955, "Formation of Vertical Fractures by Means of Highly Viscous Fluids," in *Proc., 4th World Petroleum Congress*, pp. 579–586.
[13] Nordgren, R., 1972, "Propagation of Vertical Hydraulic Fractures," SPEJ, **12**, pp. 306–314.
[14] Perkins, T. K., and Kern, L. R., 1961, "Widths of Hydraulic Fractures," J. Pet. Technol., **222**, pp. 937–949.
[15] Detournay, E., and Garagash, D. I., 2004, "General Scaling Laws for Fluid-Driven Fractures," Preprint.
[16] Spence, D. A., and Sharp, P., 1985, "Self-Similar Solutions for Elastohydro Dynamic Cavity Flow," Proc. R. Soc. London, Ser. A, **400**, pp. 289–313.
[17] Desroches, J., Detournay, E., Lenoach, B., Papanastasiou, P., Pearson, J. R. A., Thiercelin, M., and Cheng, A. H.-D., 1994, "The Crack Tip Region in Hydraulic Fracturing," Proc. R. Soc. London, Ser. A, **447**, pp. 39–48.
[18] Lenoach, B., 1995, "The Crack Tip Solution for Hydraulic Fracturing in a Permeable Solid," J. Mech. Phys. Solids, **43**(7), pp. 1025–1043.
[19] Detournay, E., and Garagash, D. I., 2003, "The Near-Tip Region of a Fluid-Driven Fracture Propagating in a Permeable Elastic Solid," J. Fluid Mech., **494**, pp. 1–32.
[20] Detournay, E., Adachi, J. I., and Garagash, D. I., 2002, "Asymptotic and Intermediate Asymptotic Behavior Near the Tip of a Fluid-Driven Fracture Propagating in a Permeable Elastic Medium," in *Structural Integrity and Fracture*, Dyskin, Hu, and Sahouryeh, eds., Swets and Zeitlinger, Lisse.
[21] Garagash, D., and Detournay, E., 2000, "The Tip Region of a Fluid-Driven Fracture Propagating in an Elastic Medium," ASME J. Appl. Mech., **67**, pp. 183–192.
[22] Detournay, E., 2004, "Propagation Regimes of Fluid-Driven Fractures in Impermeable Rocks," Int. J. Geomech., **4**, pp. 1–11.
[23] Adachi, J. I., and Detournay, E., 2002, "Self-Similar Solution of a Plane-Strain Fracture Driven by a Power-Law Fluid," Int. J. Numer. Analyt. Meth. Geomech., **26**, pp. 579–604.
[24] Carbonell, R. S., Desroches, J., and Detournay, E., 1999, "A Comparison Between a Semi-Analytical and a Numerical Solution of a Two-Dimensional Hydraulic Fracture," Int. J. Solids Struct., **36**, pp. 4869–4888.
[25] Savitski, A. A., and Detournay, E., 2002, "Propagation of a Penny-Shaped Fluid-Driven Fracture in an Impermeable Rock: Asymptotic Solutions," Int. J. Solids Struct., **39**, pp. 6311–6337.
[26] Garagash, D. I., and Detournay, E., 2005, "Plane-Strain Propagation of a Fluid-Driven Fracture: Small Toughness Solution," ASME J. Appl. Mech., **72**, pp. 916–928.
[27] Adachi, J. I., and Detournay, E., 2005, "Plane-Strain Propagation of a Fluid-Driven Fracture: Finite Toughness Self-Similar Solution," (in preparation).
[28] Garagash, D. I., 2005, "Plane-Strain Propagation of a Hydraulic Fracture During Injection and Shut-In: Asymptotics of Large Toughness," Eng. Fract. Mech., **73**(4), pp. 456–481.
[29] Adachi, J. I., and Detournay, E., 2006, "Propagation of a Fluid-Driven Fracture in a Permeable Medium," Int. J. Fract. (submitted).
[30] Garagash, D. I., 2000, "Hydraulic Fracture Propagation in Elastic Rock with Large Toughness," in *Proc. 4th North American Rock Mechanics Symp.*, J. Girard, M. Liebman, C. Breeds, and D. T, eds., pp. 221–228.
[31] Adachi, J. I., 2001, "Fluid-Driven Fracture in Permeable Rock," PhD. thesis, University of Minnesota, Department of Civil Engineering (available at www.umi.com), December.
[32] Mitchell, S. L., Kuske, R., and Peirce, A. P., 2005, "An Asymptotic Framework for Finite Hydraulic Fractures Including Leak-Off," to SIAM J. Appl. Math. (under review).
[33] Mitchell, S. L., Kuske, R., Peirce, A. P., and Adachi, J. I., 2005, "An Asymptotic Analysis of a Finger-Like Fluid-Driven Fracture," (in preparation).
[34] Griffith, A. A., 1921, "The Phenomena of Rupture and Flow in Solids," Philos. Trans. R. Soc. London, Ser. A, **221**, pp. 163–198.
[35] Martin, P. A., 1991, "End-Point Behavior of Solutions to Hypersingular Integral Equations," Proc. R. Soc. London, Ser. A, **432**, pp. 301–320.
[36] Garagash, D. I., 2005, "Propagation of a Plane-Strain Hydraulic Fracture With a Fluid Lag: Early Time Solution," Int. J. Solids Struct. (in press).
[37] Lecampion, B., and Detournay, E., 2006, "An Implicit Algorithm for the Propagation of a Hydraulic Fracture With a Fluid Lag," Computer Methods in Applied Mechanics and Engineering (submitted).